

Distribution of the Ratio of Consecutive Level Spacings for Any Symmetry and Arbitrary Degree of Chaos

A. L. Corps¹ and A. Relaño^{2,*}

¹*Departamento de Estructura de la Materia, Física Térmica y Electrónica,
Universidad Complutense de Madrid, Av. Complutense s/n, E-28040 Madrid, Spain*
²*Departamento de Estructura de la Materia, Física Térmica y Electrónica and GISC,
Universidad Complutense de Madrid, Av. Complutense s/n, E-28040 Madrid, Spain*

(Dated: October 4, 2019)

Theoretical expressions for the distribution of the ratio of consecutive level spacings for quantum systems with transiting dynamics remain unknown. We propose a family of one-parameter distributions $P(r) \equiv P(r; \beta)$ that models the evolution of the regularity class of a quantum system characterized by any symmetry and with an arbitrary degree of chaos, and show that the reduction of such a family to a universal formula, albeit desirable, is not possible. Stringent numerical calculations with the classical random ensembles and real physical systems permits us to suggest a particular ansatz for all three Poisson-GOE, Poisson-GUE, and GOE-GUE transitions, with a negligible associated error in typical situations. This enables a convenient and systematic study of quantum chaos with this spectral statistic in a vast range of practical scenarios.

I. INTRODUCTION

Quantum chaos has been of the utmost importance during the last and present century. The unraveling of how this type of behavior in the quantum realm emerges from classical mechanics would help us delve deeper into the correspondence principle that ties both interpretations of reality together.

On the one hand, classical chaos has been currently explored to a great extent and is solidly substantiated both by phenomenological and mathematical theories [1]. While we are still lacking a precise definition of the term, classical chaos is often referred to as a hypersensitivity of the time evolution of the system to vanishingly small differences in the initial conditions, as is frequently exemplified, for instance, with tools such as the Lyapunov exponents that quantify an exponential divergence between them. The onset of classical chaos from the regular regime is unambiguously resolved by the KAM theory [2], which determines how the previous invariant tori in phase space, on which the motion takes place, get continuously destroyed. On the other hand, for the quantum counterpart, the uncertainty principle invalidates any characterization in terms of physical trajectories. To make matters worse, the unitarity of the time-evolution operator, usually explicitly taken as an axiom for the quantum theory, means it becomes hopeless to expect any kind of separation between states. To warp it up, any possible analogy with classical dynamics gets completely shattered by the absence of functionally independent constants of motion [3].

A smooth generalization from classical to quantum chaos is simply impossible. The pioneering work of Berry and Tabor in the 1970s [4] states that for quantum Hamiltonians whose classical analog is integrable the

level statistics and their fluctuations properties alike follow a simple Poisson law. The transition from integrability to chaos is found to be mediated by a universally shared dramatic change in the eigenlevel statistics [5].

In the mid-1950s, Wigner [6, 7] was compelled to make use of Random Matrix Theory (RMT) [8] in order to devise a dynamical model of the atomic nucleus, for which no mathematical theory was known. He was then followed by Dyson [9] and others. The process involved assuming that the behavior of any *complicated* many-body system could be understood by means of a mathematical representation that was no less than a random matrix with the only condition that it should accommodate the various symmetries of the system under consideration.

Around 1984 one particular event led to an exponential development of both the RMT and quantum chaos: the final link between RMT and the spectral fluctuation properties of quantum systems with a chaotic classical analog. The work of Bohigas, Giannoni, and Schmit yielded the famous conjecture that bears their names [10]. The BGS conjecture essentially makes the bold statement that level fluctuations of those quantum systems whose classical analogs chaotic will fall into the descriptions of one of the three classical random ensembles, these being the Gaussian Orthogonal Ensemble (GOE), the Gaussian Unitary Ensemble (GUE), and the Gaussian Symplectic Ensemble (GSE), and establishes the symmetries present in the Hamiltonian at hand as the one and only variable that preserves the individuality of each quantum chaotic system through an analysis based merely on statistical considerations. This new systematic method of studying quantum chaos consisted in an identification of energy level fluctuation properties of a given quantum system and the behavior of its classical analog for large time scales [11]. It is remarkable that to date, only non-generic counterexamples, such as arithmetic billiards, are known to violate this conjecture [12]. Explanations for the conjecture in the semiclassical limit have been suggested [13]. Its usefulness has become increasingly acknowledged by

* armando.relano@fis.ucm.es

an important amount of radically different fields [14–19].

Random matrix ensembles (RME) describe energy levels of real systems at a statistical level, but this is true *only* when taking a local energy window in which the mean level density is set to unity. For these statistical properties to be accurately compared with the predictions of RMT, the above requirement is of vital importance. A transformation called unfolding needs to be performed to fulfill the requirement, which consists in mapping the system eigenlevels by means of the smooth (continuous) part of the density of states. Therefore, the knowledge of the system density of energy states is required. In principle, this quantity can be –and often is– wildly dependent on each physical system, and it is not uncommon to not know the structure of such a function. Also worth mentioning is the realization that an unfolded spectrum can be a victim of numerous non-negligible spurious effects that manifest throughout its entirety [20, 21]. It is, then, desirable for one to seek alternatives for which the unfolding procedure plays no role whatsoever.

One of such tools, on which we focus in this work, is the *distribution of the ratio of consecutive level spacings*, $P(r)$, which has been growing in popularity since its introduction to the scientific community [22], immensely propelled by the derivation of theoretical expected values for the Poisson, GOE, GUE, and GSE cases only in 2013 [23] as well as the transparency of the analysis it provides. Most physical systems, however, cannot be fully taken into account by any one of those regularity limits due to their intrinsic nature of *intermediate* dynamics. This makes it easy to understand why one needs to obtain results for those cases where the *degree of chaoticity* is not clear and needs to be assessed. Whether these transitions can be characterized by results that promise universality is another non-trivial question in its own right. So far, one model for the GOE-GUE transition has been exactly derived [24]. For the Poisson-GOE transition, a heuristic suggestion for a particular system has also been proposed before [25], and an attempt to analytically solve the problem has been made as well [26]. Even though these findings can and must indeed be understood as clear progress, it should be noted that it does not exonerate them from suffering from the important shortcoming that, as we show in this work, there does not exist, *and there cannot exist*, a universal result that allows for the interpolation between regularity and symmetry classes for an infinite range of arbitrary systems.

This paper is organized as follows. In Sec. II we summarize the main results of our work and give useful information regarding our crossover distribution. In Sec. III we give details on the mathematical structure of our formula. In Sec. IV we show our distribution reduces the error with respect to the theoretical GOE and GUE expressions given in [23]. In Sec. V we apply our distribution to analyze the Poisson-GOE crossover in four different systems and propose practical ansatzs. In Sec. VI we display results for the less common Poisson-GUE and GOE-GUE crossovers. Finally, in Sec. VII we gather

the main conclusions of the previous sections.

II. SUMMARY OF MAIN RESULTS

In this section we aim to give the practical results of our work in a summary format. A detailed discussion on all of them can be found in subsequent sections.

Crossover distribution. Our main result is the one-parameter distribution for the ratio of consecutive level spacings spectral statistic

$$P(r; \beta, \gamma(\beta)) = C_\beta \frac{(r + r^2)^\beta}{[(1 + r)^2 - \gamma(\beta)r]^{1+3\beta/2}}. \quad (1)$$

Here, β determines the degree of chaos of the system. $\gamma(\beta)$ is a system-dependent function of the degree of chaos and determines the precise shape of the distribution. As we will discuss in detail later, *it is not possible to find a universal $\gamma(\beta)$ covering all generic crossovers from integrability to chaos*. However, it is possible to construct a practical ansatz, valid for the majority of typical situations. Finally, the normalization constant C_β is calculated via the condition $\int_0^\infty dr P(r; \beta) = 1$.

Useful constants and ansatzs. In Table I, we summarize the main results for integrable and fully chaotic systems yielded by our distribution Eq. (5). It is worth remarking that our results for $\langle r \rangle$ and $\langle \tilde{r} \rangle$, where \tilde{r} is the random variable taking on values $\tilde{r}_n \equiv \min\{r_n, 1/r_n\}$ distributed over $[0, 1]$ with distribution $P(\tilde{r}) = 2P(r)\Theta(1 - r)$, for GOE and GUE are slightly different from the analytical results reached in [23]. The latter are obtained from 3×3 random matrices; ours introduce small corrections to better describe fits of numerical data.

Quantity	Poisson	GOE	GUE
β	0	1	2
$\gamma(\beta)$	0	$\frac{4}{5}$	$\frac{8}{9}$
C_β	1	$\frac{96}{25}$	≈ 12.6532
$\langle r \rangle$	∞	$\frac{9}{5}$	≈ 1.37584
$\langle \tilde{r} \rangle$	$\ln 4 - 1$	$5 - 2\sqrt{5}$	≈ 0.59769

TABLE I. Calculated values of the useful quantities β , $\gamma(\beta)$, C_β , $\langle r \rangle$, and $\langle \tilde{r} \rangle$ for the crossover distribution Eq. (1) in the Poisson, GOE, and GUE limits.

In Table II, we suggest practical ansatzs for Poisson-GOE, Poisson-GUE, and GOE-GUE crossovers. As we

will show later, they typically incur in significant errors so long as one considers around 10^3 ratios.

Transition	β	$\gamma(\beta)$
Poisson-GOE	$0 \leq \beta \lesssim 1$	$\frac{4}{5} [5\beta^4 - 4\beta]$
Poisson-GUE	$0 \leq \beta \lesssim 2$	$\frac{8}{9} \left[5 \left(\frac{\beta}{2} \right)^4 - 4 \left(\frac{\beta}{2} \right) \right]$
GOE-GUE	$1 \lesssim \beta \lesssim 2$	$\frac{4}{45}\beta + \frac{32}{45}$

TABLE II. Functional structure chosen for $\gamma(\beta)$ for different transitions involving the Poisson, GOE, and GUE classical random ensembles.

III. CROSSOVER DISTRIBUTION

In this section we define the probability density function used in this work, detail the assumptions made in order to reach it, and briefly comment on some of its most relevant mathematical aspects.

The ratio of consecutive level spacings is a random variable r taking on values

$$r_n \equiv \frac{s_n}{s_{n-1}}, \text{ where } s_n \equiv E_{n+1} - E_n, \forall n \in \{2, \dots, N-1\}, \quad (2)$$

and $\{E_n\}_{n=1}^N$ is a complete set of energies in ascending order, that is, verifying $E_n \geq E_m$ whenever $n \geq m$. Since the distribution of r and that of $1/r$ are the same [23], it follows that any probability density describing this random variable must fulfill the condition

$$P(r) = \frac{1}{r^2} P\left(\frac{1}{r}\right). \quad (3)$$

In a spirit similar to that of the Wigner surmise, a formula for the ratio distribution of two consecutive spacings was obtained by analytically solving the 3×3 problem associated to each of the classical random ensembles, that is, Poisson, GOE, GUE, and GSE. This probability density exhibits the exact same level repulsion as the Nearest Neighbor Spacing Distribution (NNSD) for vanishingly small values of r ; explicitly, $P(r) \sim r^\beta$ for $r \rightarrow 0$. It is only natural to follow the same intuition to now suggest an expression that interpolates between different regularity classes for a quantum system displaying different symmetries. In other words, we will ask our interpolating function to yield the correct theoretical limits when the parameter is fixed to the corresponding value. With the previous discussion we are led to propose, in analogy with the Brody distribution [27] for the NNSD, the probability density function

$$P : [0, +\infty) \rightarrow [0, +\infty) \quad (4)$$

given by

$$P_{\gamma\beta}(r) \equiv P_{\gamma\beta}(r; \beta, \gamma(\beta)) = C_\beta \frac{(r + r^2)^\beta}{[(1+r)^2 - \gamma(\beta)r]^{1+3\beta/2}}. \quad (5)$$

Here, $\beta \in [0, +\infty)$ is taken to be a non-negative, continuous parameter that describes both the regularity class (integrable or chaotic) and the symmetry associated to the system. The values $\beta = 0, 1, 2, 4$ correspond to Poisson, GOE, GUE, and GSE ensembles, respectively. $\gamma \equiv \gamma(\beta)$ is any one-variable function of β that univocally establishes the maximum of $P(r)$ at each value of β . The analytical results of [23] are recovered if

$$\gamma(\beta = 0) = 0, \quad \gamma(\beta = 1, 2, 4) = 1. \quad (6)$$

Here we note, however, that Eq. (6) will *not* be strictly fulfilled, since the original results were calculated from 3×3 random matrices, and therefore deviations from Eq. (6) are expected for larger systems. Indeed, results summarized in Table I are slightly different, but best suited for the typical matrix sizes, thus affording better results for data analysis.

Since $P(r)$ is a probability density function, it must verify $P(r; \beta, \gamma(\beta)) \geq 0, \forall r, \beta \in [0, +\infty)$. This leads to the condition

$$\gamma(\beta) < \min_{r \in [0, +\infty)} \frac{(1+r)^2}{r} = 4, \quad \forall \beta \in [0, +\infty), \quad (7)$$

which in turn ensures the non-singularity of $P(r)$, $\forall r \in [0, +\infty)$.

Here we draw attention to the nature of the γ function just defined. One could perhaps have no reason to initially choose it as a one-variable one and such a decision could in fact seem highly arbitrary. Indeed, nothing seems to prevent it from being a real n -variable function, or from being independent of β altogether. However, since the transitions we will be considering in this work are actually mediated by a single perturbative parameter, this is the choice that makes the most sense both physically and mathematically. For if it happened to be otherwise, our model Eq. (5) would also depend on more than one parameter, while the regularity class of the systems we analyze will clearly change as the value of only one parameter is varied. Any extra parameter dependence in our formula would then leave a conceptual gap with an information that corresponds to nothing in particular. This issue will be discussed further afterwards.

Finally, the normalization constant C_β is, of course, implicitly determined by the condition $\int_0^\infty dr P(r; \beta) = 1, \forall \beta \in [0, +\infty)$. Eq. (5) is the initial transiting model of our work.

It is interesting to observe how Eq. (5) behaves asymptotically, which determines the structure of level repulsion [28]. In the domain $r \ll 1$, expanding at $r = 0$ affords the Maclaurin representation

$$\begin{aligned} P(r) &\simeq C_\beta r^\beta \left[1 + (-2 - 2\beta + \gamma + \frac{3\beta\gamma}{2})r + \mathcal{O}(r^2) \right] \\ &= C_\beta r^\beta + \mathcal{O}(r^{\beta+1}), \end{aligned} \quad (8)$$

as expected. Similarly, for large values of r one has

$$P(r) \sim C_\beta \frac{r^{2\beta}}{r^{2+3\beta}} = C_\beta r^{-(2+\beta)}. \quad (9)$$

It may be useful to note that the statistical moments given by the density Eq. (5) strongly depend on the value of β and do not always exist. Indeed, let $k \in \mathbb{N}$. Then, the k -th moment of the random variable r is determined as

$$\begin{aligned} \langle r^k \rangle_\beta &\equiv \int_0^\infty dr r^k P(r; \beta) \sim \int_0^\infty dr r^{-(2+\beta-k)} < \infty \\ &\iff \beta > k - 1, \quad \forall \beta \in [0, +\infty). \end{aligned} \quad (10)$$

This means that our model does not yield a finite mean value $\langle r \rangle_{\beta=0}$ for Poisson, GOE does have a $\langle r \rangle_{\beta=1}$ but not variance, and so on. Thus, Eq. (5) successfully reproduces the same qualitative behavior with respect to the existence of moments as the original distribution for the classical random ensembles. In fact, Eq. (5) slightly improves on the mean values for r , when these exists, and those for \tilde{r} (see Table I for details) with respect to the traditional ones [23]. Note, however, that as $\beta \rightarrow 0$, $\langle r \rangle$ is badly conditioned, and for it to converge for values $0 < \beta \ll 1$ very large statistics are called for. This inconvenience is of course avoided by $\langle \tilde{r} \rangle$, which exhibits no singular behavior at any point.

Because no explicit expression for $\gamma(\beta)$ can be deduced, in what follows we will be performing non-linear fits that treat β and γ on an equal footing, that is, as unknown, independent parameters. If not necessary, we will also require our fits to find the value of the normalization constant C_β , which results in a three-parameter non-linear fit. This will *always* implicitly be the case, although at times we will refer to a two-parameter fit to mean that all three quantities are obtained.

IV. THE CHAOTIC CASE

In this section we show that our proposed model, Eq. (5), can be used to accurately describe the distribution of ratios for both the non-transiting GOE and GUE cases. These reflect the most common and ubiquitous symmetries found in physical systems, hence its relevance.

The Wigner-like surmises that we take as theoretical expected values for each of the regularity and symmetry classes –that is, the simple Poisson result and Eq. (11) for GOE ($\beta = 1$), GUE ($\beta = 2$), and GSE ($\beta = 4$)– were explicitly derived with the exact calculation for 3×3 random matrices for each of the ensembles [23], and its applicability has been extended to arbitrary dimension in a similar fashion to that of Wigner’s results. It can be checked that our one-parameter surmise perfectly reproduces the 3×3 statistics, as was to be expected. However, the latter is unluckily not the most relevant scenario for the majority of applications.

A. The GOE limit

To determine the accuracy of our model, we now go on to examine how well it can be used to describe an ensemble of $M = 10^6$ GOE random matrices each providing a number of $N = 10^3$ ratios. The corresponding histogram associated to the $P(r)$ for this situation as well as our model fit can be found in Fig. 1. These are visually indistinguishable. Since the distribution queue is so unnecessarily long for this statistic, we have decided to plot the values of $P(r)$ with $r \in [0, 5]$, which is a range that we deem reasonable. The non-linear fit we perform for Eq. (5) produces $\beta = 1.033(4)$ and $\gamma = 0.8036(9)$. The ansatz proposed in Table I has been chosen in accordance with this result. Both β and γ actually depend on the system size and, consequently, it is not very logical to set the exact results of our fit as a general ansatz.

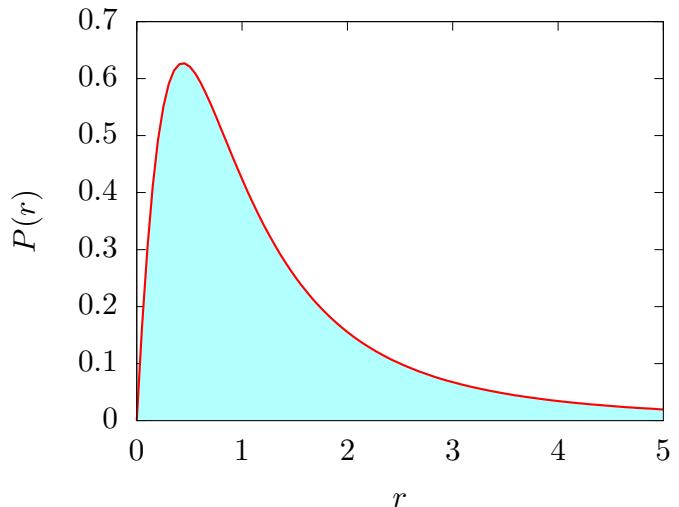


FIG. 1. (Color online) Distribution of the ratio of two consecutive level spacings, $P(r)$, calculated with an ensemble of $M = 10^6$ GOE matrices giving rise to $N = 10^3$ ratios each (blue histogram), and non-linear fit of our model $P_{\gamma\beta}(r)$, Eq. (5) (red, solid line).

We now assess how good our estimate is in terms of difference between the simulated data and the results predicted by the theoretical value given by the Wigner-like surmise that we denote from now onwards

$$P_W(r; \beta = 1, 2, 4) \equiv C_\beta \frac{(r + r^2)^\beta}{(1 + r + r^2)^{1+3\beta/2}}, \quad (11)$$

where $\beta \in \{1, 2, 4\}$ correspond to GOE, GUE, and GSE, respectively. Here we are by all means interested in $P_W(r; \beta = 1)$. To give a measure of such, we calculate

$$\delta P_i(r) \equiv |P_H(r) - P_i(r)|^2, \quad \forall r \in [0, 5], \quad (12)$$

where $P_H(r)$ denotes the distribution of ratios of given by the numerical histogram, and $P_i(r)$, with $i \in \{W, \gamma\beta\}$

represents the Wigner-like distribution, $P_W(r)$, obtained from 3×3 matrices and the result of our fit, $P_{\gamma\beta}(r)$, to Eq. (5). The results are plotted in Fig. 2. The main conclusion is that, while for values of r in the distribution queue, $2 \lesssim r \leq 5$, the differences between theoretical value and our surmise are clearly minimal, for values $0 \leq r \lesssim 2$ this is no longer the case at all. Our model reproduces the histogram values with much more accuracy than the theoretical surmise, which suffers from the inescapable fact that it was initially derived for 3×3 random matrices. This is most relevant because it is in this range of ratio values that the structure of levels repulsion is determined, for which our model would then yield better results as well.

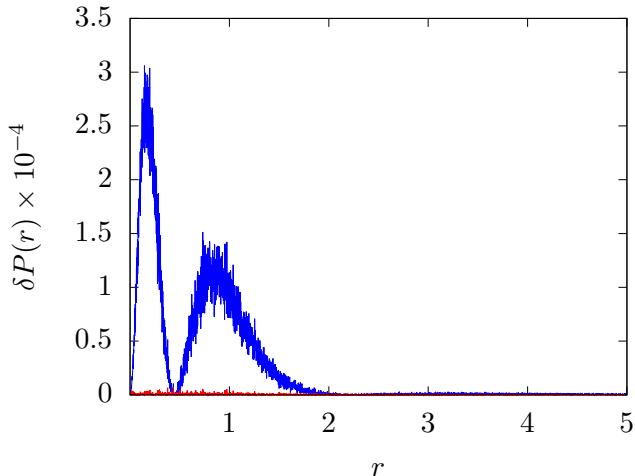


FIG. 2. (Color online) Difference $\delta P(r)$ between simulated histogram coming from $M = 10^6$ GOE random matrices providing a number of $N = 10^3$ ratios each with theoretical expected values $P_W(r; \beta = 1)$, Eq. (11) (blue, solid line), and our interpolating surmise $P_{\gamma\beta}(r)$, Eq. (5) (red, solid line).

B. The GUE limit

Quantum chaotic systems are not rare to manifest with a symmetry class characterized by an invariance under unitary changes. In an analogous way to the previous subsection, we now test our interpolating model at the GUE limit, that is, $P(r; \beta = 2)$, Eq. (5), and analyze the results it yields when compared with the theoretical value $P_W(r; \beta = 2)$, Eq. (11). The structure of the presentation is the exact same as before, and our findings are now displayed in Fig. 3 and Fig. 4.

In Fig. 3 we observe a perfect match of our model transiting model with the histogram associated to the distribution of the simulated ratios, as was expected. This time the double-parameter fit provides values $\beta = 2.049(1)$ and $\gamma = 0.879(1)$. Again, the ansatz proposed in Table I is a simplified version of this last result on the same grounds as for the GOE case. In Fig. 4 we

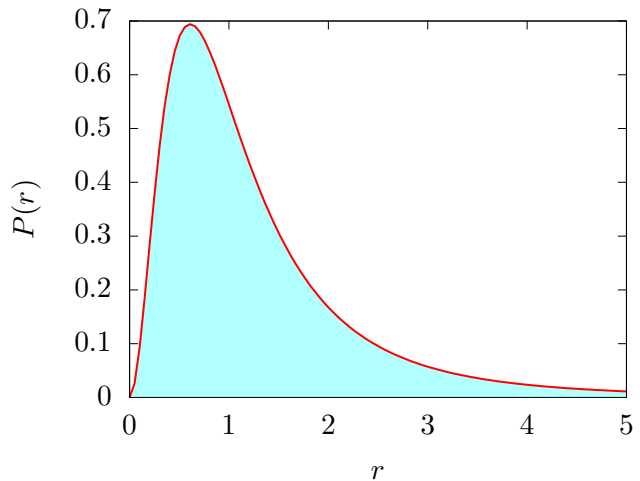


FIG. 3. (Color online) Distribution of the ratio of two consecutive level spacings, $P(r)$, calculated with an ensemble of $M = 10^6$ GUE matrices giving rise to $N = 10^3$ ratios each (blue histogram), and non-linear fit of our model, $P_{\gamma\beta}(r)$ Eq. (5) (red, solid line).

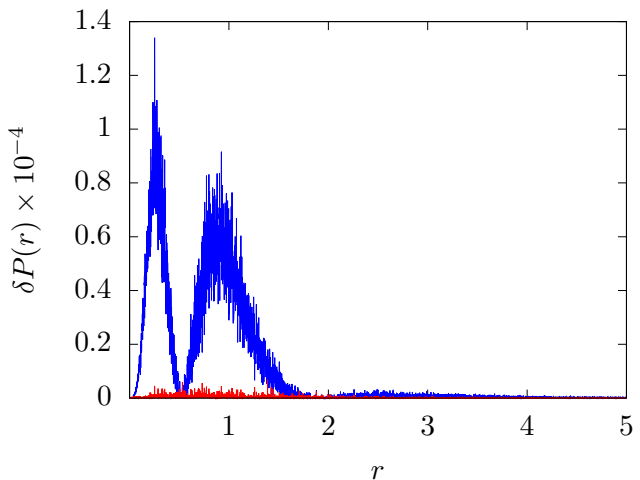


FIG. 4. (Color online) Difference $\delta P(r)$ between simulated histogram coming from $M = 10^6$ GUE random matrices providing a number of $N = 10^3$ ratios each with theoretical expected values $P_W(r; \beta = 2)$, Eq. (11) (blue, solid line), and our interpolating surmise $P_{\gamma\beta}(r)$, Eq. (5) (red, solid line).

encounter the same difference reduction with respect to the histogram that our surmise visibly provides, with the same qualitative behavior for all values of $r \in [0, 5]$. Eq. (5) proves to reduce the discrepancy with the numerical evidence when compared with the theoretical expectation.

V. TRANSITIONS FROM INTEGRABILITY TO CHAOS

Once the ability of our equation model has been checked to account for the most common symmetry limits for quantum chaotic systems, we focus on its relevance to treat transitions between these and the integrable regime. As we have already pointed out, this is of vital importance because most real physical systems cannot be described by any of the RMT classical ensemble limits, but lay in an intermediate regime. To this end, we also address the question of the universality of these transitions and find that the uniqueness of any interpolating formula of our kind is not, and in fact will never be, guaranteed. This section comprises transitions from RMT ensembles to real physical systems.

Our analysis results in an ansatz proposal for the functional form of $\gamma = \gamma(\beta)$ that depends on the kind of transition to which it can be applied. This affords a convenient expression that can be used in quite general scenarios, so long as the amount of available data does not entail a large- N limit. It must be emphasized that this represents the usual situation for most experimental investigations in complex systems, such as atoms or nuclei, as well as for many theoretical studies where the extraction of eigenlevels, of vital importance in the characterization of regularity classes, becomes seriously hindered by the exponential size scales of the Hilbert space.

A. Formulation of transiting systems

We first introduce the models in which we are interested in what follows.

I Poisson to GOE transition in RMT. This is indeed the simplest transition one can contemplate. It does not correspond to any particular physical system, and consists in explicitly and exactly generating the Poisson and GOE limits, whose matrices in each realization we denote \mathcal{H}_P and \mathcal{H}_G , respectively, and then building up the mixture state, dependent on the continuous chaoticity parameter λ , by means of the usual convex sum

$$\mathcal{H}(\lambda) \equiv \lambda \mathcal{H}_G + (1 - \lambda) \mathcal{H}_P, \quad \lambda \in [0, 1], \quad (13)$$

so that we obviously have for the limiting values $\mathcal{H}(\lambda = 0) = \mathcal{H}_P$ and $\mathcal{H}(\lambda = 1) = \mathcal{H}_G$. Other models for this transition are also possible, but this is perhaps the easiest one [29]. For our simulations, we have chosen the perturbation parameter $\lambda \in \{1.22^{q-1} \times 2 \times 10^{-6}\}_{q=1}^{51}$. A number of realizations $M = 2000$ has been performed and the matrix size for each of them is $N = 1716$.

II Poisson to GOE transition in the β -ensemble. Also known as the Continuous Gaussian Ensemble, this generalization of the classical Gaussian ensembles was in its origins studied as a theoretical joint eigenvalue

distribution with applications, for instance, in lattice gas theory [30]. It has been relatively recently found that this eigenvalue distribution can be derived from an ensemble of random matrices [31]. The Gaussian β -ensemble has since been used for various purposes [32, 33]. It has been proposed as a model to describe the many-body to localized phase transition [34], although this has been shown to be valid for short-range statistics only [21]. The ensemble essentially consists of tridiagonal, real, and symmetric matrices whose entries are classical random variables, these being normal, $\mathcal{N}(\mu, \sigma)$ with μ being its mean and $\sigma \equiv \sqrt{\sigma^2}$ its standard deviation, and chi, $\chi_k \equiv \sqrt{\chi_k^2}$ with $k \in \mathbb{R}_+ \cup \{0\}$ denoting a continuous, non-negative number of degrees of freedom. The matrix elements of the model $\mathcal{H}_{i,j} \equiv (\mathcal{H})_{i,j}$ are random variables distributed over \mathbb{R} with distribution given by

$$\mathcal{H}_{ii} \sim \mathcal{N}\left(0, \sqrt{\frac{1}{2\lambda}}\right), \quad \forall i \in \{1, 2, \dots, N\}, \quad (14)$$

and

$$\mathcal{H}_{i+1,i} = \mathcal{H}_{i,i+1} \sim \sqrt{\frac{1}{4\lambda}} \chi_{(N-i+1)\beta}, \quad \forall i \in \{1, 2, \dots, N-1\}, \quad (15)$$

with $\lambda, \in \mathbb{R}_+$, $\beta \in [0, +\infty)$ being free parameters. The values $\beta = 0, 1, 2, 4$ correspond to Poisson, GOE, GUE, and GSE, respectively, and β can take any real, positive value [35]. Here, the convention that $\chi_0 \equiv 0$ is assumed. For our simulations, we have made the simple choice $\lambda = 1$ and $\beta \in \{0.02(q-1)\}_{q=1}^{51}$. We have averaged over $M = 2000$ realizations, and the matrix size for each one of them has been taken $N = 1716$.

III Poisson to GOE transition in a Heisenberg XXZ spin-1/2 chain. This is the first example that represents a real physical system. Disordered interacting spin-1/2 chains have been used as models for quantum computers, magnetic compounds, and have been simulated in optical lattices [36–38]. The Heisenberg spin-1/2 chain has been shown to transit from integrability to chaos, for instance, with the NNSD [34, 39, 40] or the δ_n [21]. The Hamiltonian of the model is given by

$$\mathcal{H} = \sum_{n=1}^L \omega_n \hat{S}_n^z + \sum_{n=1}^{L-1} J \hat{S}_n \cdot \hat{S}_{n+1}, \quad (16)$$

where L is the number of sites and $\hat{S}_n \equiv \vec{\sigma}_n/2$ are the spin operators located at site n with $\vec{\sigma}_n$ being the Pauli spin matrices at that exact site. The first term in Eq. (16) describes effects of a static magnetic field in the z -direction. Each ω_n is a random variable distributed uniformly, $\omega_n \sim \mathcal{U}(-\omega, \omega)$. Two possible couplings between the nearest neighbor spins are described by the last term of Eq. (16). The first one is simply the diagonal Ising interaction, while the second is the off-diagonal flip-flop

term, which is responsible for excitation propagation in the chain. Also, the chain is taken to be isotropic since J is a constant that quantifies both the coupling strength between the Ising interaction and that of flip-flop term. Only two-body interactions can take place in this chain.

For our simulation, we have taken $J = 1$, $\hbar \equiv 1$, and $L = 13$. We have generated 50 different cases, with $\omega \in \{0.2q\}_{q=1}^{50}$. Since $[H, \hat{S}_z] = 0$, we consider the sector with $\hat{S}_z = -1/2$. In this case, the dimension of the Hilbert space is $d = \binom{13}{6} = 1716$. The size of each spectrum has been therefore chosen $N = 1716$, and we have simulated $M = 2000$ realizations.

IV Poisson to GOE transition in a Gaudin elliptic model. In contrast with the XXZ chain, this model is based on long-range interactions between spin-1/2 magnets. It is the most general of a family of exactly solvable models derived from a generalized Gaudin algebra, which includes the Bardeen-Cooper-Schrieffer, the Suhl-Matthias-Walker, the Lipkin-Meshkov-Glick, the generalized Dicke, and nuclear interacting boson models, to quote but a few [41]. Its XXZ version includes three different integrable classes (rotational, trigonometric, and hyperbolic). The rotational class one is known to coincide with the classical BCS mean-field solution in the thermodynamical limit [42]. Here, we work with its XYZ version, which has been previously studied in [43] and can be written

$$\mathcal{H} = \sum_i \epsilon_i R_i, \quad (17)$$

where ϵ_i are free parameters, and R_i are two-spin operators of the form

$$R_i \equiv \sum_{j=1, i < j}^d \tilde{X}_{i,j} \sigma_i^x \sigma_j^x + \tilde{Y}_{i,j} \sigma_i^y \sigma_j^y + \tilde{Z}_{i,j} \sigma_i^z \sigma_j^z, \quad (18)$$

with $\sigma^x, \sigma^y, \sigma^z$ being the Pauli matrices. The matrices \tilde{X} , \tilde{Y} , and \tilde{Z} can be chosen to induce a complete transition from integrability to fully developed chaos via a single-parametric perturbation. Following the proposal in [43] we choose

$$\begin{aligned} \tilde{X}_{j,k} &= (\cos \alpha) X_{j,k} + (\sin \alpha) A_{j,k}, \\ \tilde{Y}_{j,k} &= (\cos \alpha) Y_{j,k} + (\sin \alpha) B_{j,k}, \\ \tilde{Z}_{j,k} &= (\cos \alpha) Z_{j,k} + (\sin \alpha) C_{j,k}. \end{aligned} \quad (19)$$

The matrices

$$\begin{aligned} X_{j,k} &= \frac{1 + \kappa \operatorname{sn}^2(z_j - z_k)}{\operatorname{sn}(z_j - z_k)}, \\ Y_{j,k} &= \frac{1 - \kappa \operatorname{sn}^2(z_j - z_k)}{\operatorname{sn}(z_j - z_k)}, \\ Z_{j,k} &= \frac{\operatorname{cn}(z_j - z_k) \operatorname{dn}(z_j - z_k)}{\operatorname{sn}(z_j - z_k)}, \end{aligned} \quad (20)$$

with $z_j \in \mathbb{R}$, $j \in \{1, \dots, N\}$, being free parameters, $\operatorname{sn}(x) \equiv \operatorname{sn}(x, \kappa)$ is the Jacobi elliptic function of modulus $\kappa \in [0, 1]$, and cn and dn are related by $d \operatorname{sn}(x)/dx = \operatorname{cn}(x) \operatorname{dn}(x)$, give rise to an integrable model, which can be solved by Bethe ansatz [44]. If $\alpha = 0$, all the R matrices commute pairwise, $[R_i, R_j] = 0$, $\forall i \neq j$, and thus the system has as many integrals of motion as degrees of freedom.

The remaining set of matrices are used to break the integrability of the model. They are chosen as

$$\begin{aligned} A_{j,k} &= \mu + \sigma \cos \left[\sqrt{2\lambda}(\omega_j - \omega_k) \right], \\ B_{j,k} &= \mu + \sigma \cos \left[\sqrt{3\lambda}(\omega_j - \omega_k) \right], \\ C_{j,k} &= \mu + \sigma \cos \left[\sqrt{5\lambda}(\omega_j - \omega_k) \right], \end{aligned} \quad (21)$$

with $\lambda, \omega_j \in \mathbb{R}$ being free parameters, μ being the average of all matrix elements of A , B , and C , and σ is the standard deviation associated with it. The transiting parameter α takes values $\alpha \in [0, \pi/2]$, in such a way that for $\alpha = 0$ the system is completely regular and for $\alpha = \pi/2$ it is completely chaotic. The simulation consists of $M = 3000$ realizations of chains with $d = 11$ spins, each one giving rise to a system of dimension $N = 2^{10} = 1024$, due to the presence of a discrete symmetry. As it has been shown [43] that the transition to chaos is completed around $\alpha \sim \pi/4$, we choose $\alpha \in \{\pi q/200\}_{q=1}^{60}$.

B. Universality of the transitions

Here we present and comment on the results yielded by our simulations of the systems previously introduced.

One of the questions that needs to be addressed about our transiting model Eq. (5) is the existence of a functional form for $\gamma = \gamma(\beta)$ that might be applicable to any generic physical system. The simulated data provides all we need to construct the distribution of the ratio of two consecutive level spacings, Eq. (2), via the diagonalization of the Hamiltonian of each transition. For each one of them, and for each value of the perturbative parameter therein, we proceed with a non-linear fit of our equation $P(r; \beta, \gamma(\beta))$ for the distribution given by the histograms, $P_H(r)$. The equality of the bin sizes means that the results can be legitimately put in comparison. The results are shown in Fig. 5.

Panel (a) of Fig. 5 plays the role of supplying a clear refutation of the possibility of a universal transiting formula for the ratios distribution, since one such expression would need to describe the behavior of systems that exhibit not only quantitatively but also qualitatively very different evolutions. As can be seen, there exists no easy way to characterize these four curves at the same time. We observe two qualitatively different curves when we examine how the particular transition has been generated: the transition associated to the system II, that is, the

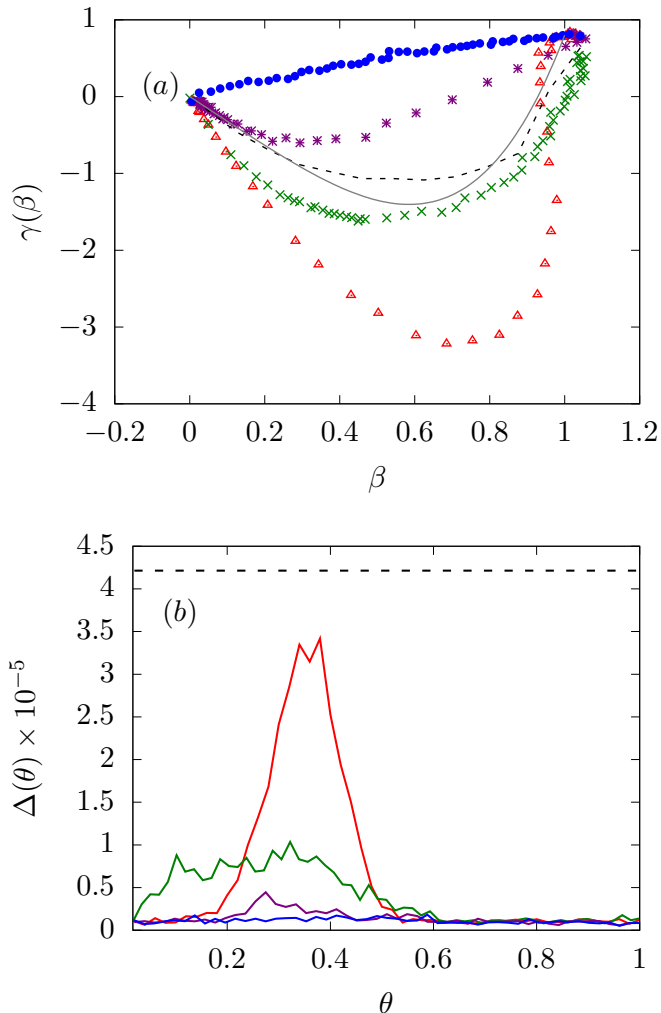


FIG. 5. (Color online) Panel (a): Best non-linear double-fit result $\gamma = \gamma(\beta)$ for the distribution of the ratio of two consecutive level spacings simulated for the Poisson-GOE transition in RMT (red triangles), the β -ensemble (blue circles), a Heisenberg spin-1/2 chain (purple * symbols), and the Gaudin elliptic model (green \times symbols). Plotted against them are the global average of data (black, dashed line) and our proposed ansatz for the Poisson-GOE crossover (grey, solid line). Panel (b): Representation of Eq. (23) for the corresponding curves. In this case, we have plotted the result this procedure would yield when applied to the last (GOE) value of the β -ensemble model (black, dashed line) to set an upper limit.

β -ensemble, is slightly concave; analogously, the curves that correspond to the remaining systems I, III, and IV, although not so much quantitatively, share a qualitative commonality in that both of them are convex. These two groups of functions are obviously mutually exclusive. In addition, once the general shape has been accounted for, these last three curves have nothing in common with each other. In passing we note that although $\gamma(\beta)$ is multivalued for $0.9 \lesssim \beta \lesssim 1$, this is entirely due to fluctuations

and should not be a source of alarm. In addition, we have plotted an average of all four curves, which we show with a dotted line. Finally, we plot with a grey solid line the ansatz for the Poisson-GOE crossover given in Table II, a fit of a choice that allows to approximately parametrize $\gamma(\beta)$ for the systems that we consider here. It should be noted that, in general, these curves are quite difficult to parametrize in terms of simple functions. Even more so if one contemplates parametrizing all four curves with a family of simple functions.

In order to determine the goodness of Eq. (5), we calculate the difference between the best fit to this equation and the numerical histogram for each of the systems we consider here. To this end, we consider a partition of the interval under consideration $[0, 5]$ given by

$$\mathcal{P}([0, 5]) \equiv \{[\delta r(i-1), \delta r(i)]\}_{i=1}^n, \quad (22)$$

where δr is, as usual, the bin size in the histogram and is such that $\delta r \times n = 5$. Then the number $n \in \mathbb{N}$ can be interpreted as the *number of bins* employed in our analysis. For each interval in the partition Eq. (22), we consider the i -th mid-point $r_i \equiv (2i-1)\delta r/2 \in [0, 5]$, $i \in \{1, 2, \dots, n\}$. If we let $P^{(q)}(r)$ denote the distribution of the ratio of consecutive level spacings for the q -th value of the transition parameter, then the number

$$\Delta(q) \equiv \frac{1}{n} \sum_{j=1}^n \left| P_H^{(q)}(r_j) - P_i^{(q)}(r_j) \right|^2, \quad \forall q \in \{1, 2, \dots, q_{\max}\}, \quad (23)$$

and $i \in \{\gamma, \beta, W\}$, represents the squared difference between the histogram values and the distribution fits at each point r_i averaged over the total number of bins. This representation can be used to measure the discrepancy between simulated data in the transition and our models. Note that Eq. (23) supplies results that are effectively independent on the number of bins. When several numbers of realizations M are taken into account to construct the distribution for each step of the transition, *all* of them must be included in Eq. (23). Since the number of parameters for the crossovers have been chosen slightly different depending on the system, we plot the results as a function of the *normalized parameter*

$$\theta \equiv \frac{q}{q_{\max}} \in [0, 1], \quad q \in \{q_{\min}, q_{\min} + 1, \dots, q_{\max}\}, \quad (24)$$

where q_{\max} (q_{\min}) is the highest (lowest) value of q for each system. This allows us to put all the results in comparison.

In panel (b) of Fig. 5, we plot the results of Eq. (23) applied to the fits displayed in panel (a) of the same figure. For reference, we also show, with a black, dashed line, the error between the numerical GOE and the theoretical expression $P_W(r; \beta = 1)$, Eq. (11), given in [23]. As can be seen, Eq. (5) produces less error than Eq. (11) even when made use of with a two-parameter fit.

Under these circumstances, it becomes apparent that there cannot exist a unique $\gamma(\beta)$ that serves the ambitious purpose of entirely taking into account all possible

systems with intermediate dynamics, i.e. many such formulae could in principle be found but *they would be valid only for that system for which it was explicitly derived*. The one-variable choice for the structure of $\gamma(\beta)$ is incidentally reinforced by the results of Fig. 5, where a reasonably smooth plot can be observed for all four transitions. The compatibility of this remark with a possible but still unlikely scenario where γ might be sensitive to some other parameter besides β reveals to be doubtful.

In Fig. 6, we show how our general surmise Eq. (5) works very well to describe crossovers with high statistics. This is exemplified by means of the Heisenberg spin chain XXZ model. Quantitative numerical results for the best non-linear double-fit are shown in Table III, where we observe that β behaves as a monotonically increasing smooth function exhibiting very reasonable errors.

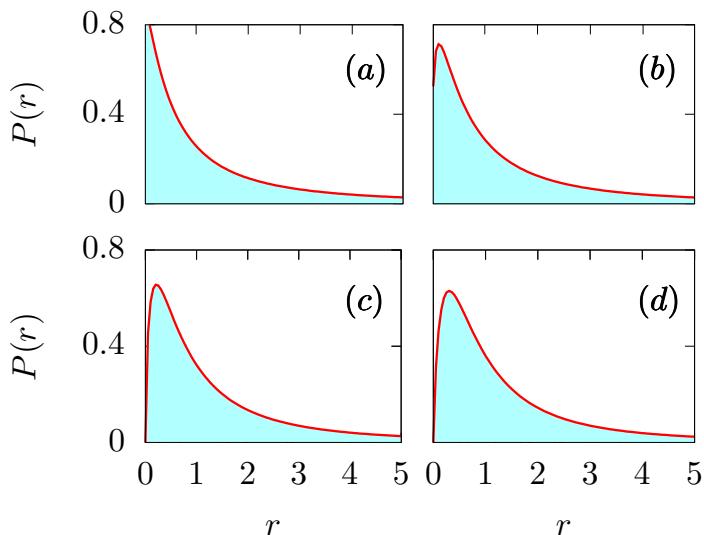


FIG. 6. (Color online) Distribution of the ratio of consecutive level spacings for the Heisenberg spin-1/2 XXZ chain model with $N = 1716$, $M = 2000$, and $\delta r = 0.05$ (blue, filled histogram), with the best non-linear fits of $P_{\gamma\beta}(r)$, Eq. (5) (red, solid line). The values of the transition parameter for panels (a) – (b) are given by $q \in \{25, 15, 12, 10\}$, respectively.

C. Ansatz proposal

Another question that deserves to be explored is the ability of our model to correctly measure the degree of chaos in a given transiting physical system by means of a double fit. Here two alternatives are initially possible:

- (i) a double-fit $\gamma - \beta$ is always applicable, and
- (ii) a compromise ansatz that requires no double-fitting is desirable.

We will first analyze the difficulties that (i) involves, and then conclude that (ii) is the best option in terms of applicability, proposing such an ansatz.

Panel	Double-fit
(a)	$\beta = 0.1010(22)$ $\gamma = -0.300(19)$
(b)	$\beta = 0.3898(44)$ $\gamma = -0.549(25)$
(c)	$\beta = 0.6038(45)$ $\gamma = -0.211(18)$
(d)	$\beta = 0.7943(50)$ $\gamma = 0.189(15)$

TABLE III. Values and uncertainties of best non-linear double-fit and with our proposed ansatz referred to panels (a) – (d) in Fig. 6.

(i) *Double-fitting shortcomings*. To this end, we show Fig. 7, where we plot Eq. (5) with the choices $\gamma(\beta = 0.453) = 1.643$ and $\gamma(\beta = 0.664) = 0.887$. These values of $\beta \notin \{0, 1\}$ lie in the interval $(0, 1)$, which is the one we associate with partially integrable or GOE chaotic dynamics, representing a situation in which assessing the regularity may not be a straightforward matter. For the values of γ , we have made two very distinct choices which in conjunction with the values of β should offer two very different representations of a system. However, we find the curves to be almost indistinguishable, and this is all the more true as $r \rightarrow 0$ and $r \rightarrow \infty$, which is the regime that determines level repulsion. This should be taken as a word of caution regarding the practice of double-fitting, which proves to be extremely sensitive to the data with which it must be in accordance. For the fit to differentiate between these two curves, we would need to have a very large set of information. This implies that casting Eq. (5) into a form for which a single-parameter fit suffices is highly desirable, since this would mean a much more robust result when one cannot obtain large statistics to analyze. Note that in this case a double-parameter fit would produce ill-defined results and under no circumstances could these be taken as representative.

(ii) *Definition of ansatz*. In essence, we now seek to rewrite Eq. (5) so as to free it from the unknown $\gamma(\beta)$, that is,

$$P(r; \beta, \gamma(\beta)) \mapsto P(r; \beta). \quad (25)$$

This transformation requires assigning $\gamma(\beta)$ an explicit form depending on β alone, for at no point has it been specified. Let us recall that it is this ambiguity that forces a much troublesome double-fit. To circumvent this inconvenience, we propose an *ansatz* for $\gamma = \gamma(\beta)$. For definiteness, our choice consists in a polynomial model since

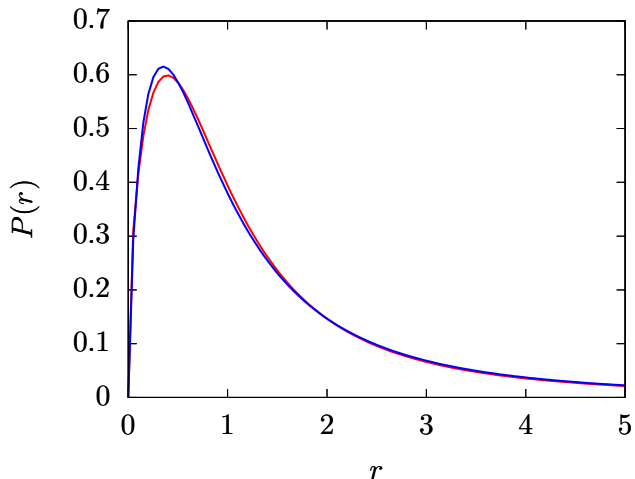


FIG. 7. (Color online) Transiting distribution of the ratio of consecutive level spacings Eq. (5) for the values $\gamma(\beta = 0.453) = 1.643$ (red, solid line) and $\gamma(\beta = 0.664) = 0.887$ (blue, solid line).

this is surely the simplest one that can fulfill the limiting condition $\gamma(\beta = 0) = 0$ and the cut-off $\gamma(\beta = 1) \approx 0.8$ for large statistics as well as approximately parametrize the curves shown in Fig. 5. For the Poisson-GOE transition, we propose

$$\gamma_{\text{P-GOE}}(\beta) = \frac{4}{5} [5\beta^4 - 4\beta], \quad (26)$$

which is the choice displayed with a solid line in panel (a) of Fig. 5.

For the Poisson-GUE transition, we have the large-statistics cut-off $\gamma(\beta = 2) \approx 8/9$, so we propose as an ansatz an extension of Eq. (26) given by

$$\gamma_{\text{P-GOE}}(\beta) = \frac{8}{9} \left[5 \left(\frac{\beta}{2} \right)^4 - 4 \left(\frac{\beta}{2} \right) \right]. \quad (27)$$

Finally, for the GOE-GUE transition the conditions $\gamma(\beta = 1) \approx 4/5$ and $\gamma(\beta = 2) \approx 8/9$ must be verified. Here we consider the non-zero intercept model $\gamma(\beta) = \delta\beta + \alpha$, with $\delta, \alpha \in \mathbb{R}$, which produces

$$\gamma_{\text{GOE-GUE}}(\beta) = \frac{4}{45}\beta + \frac{32}{45}, \quad (28)$$

which is in accordance with the GOE and GUE limits in Eq. (26) and Eq. (27), since $\gamma_{\text{GOE-GUE}}(\beta = 1) = 4/5$ and $\gamma_{\text{GOE-GUE}}(\beta = 2) = 8/9$.

When Eq. (26) ($0 \leq \beta \lesssim 1$), Eq. (27) ($0 \leq \beta \lesssim 2$), and Eq. (28) ($1 \lesssim \beta \lesssim 2$) are inserted into our distribution model Eq. (5), one obtains the desired one-parameter dependent result Eq. (25), which we shall denote $P_{\text{P-GOE}}(r)$, $P_{\text{P-GUE}}(r)$, and $P_{\text{GOE-GUE}}(r)$, respectively.

D. Application and analysis of ansatz

In this section we show our ansatz Eq. (26) can be used to correctly measure the degree of chaos as well as the symmetry class of quantum systems with intermediate dynamics via a single-parameter fit in the Poisson-GOE crossover. We analyze the role of the statistics size in the associated error and conclude that our model provides better results as the available information to perform the fit is more scarce, yielding a very small difference with respect to a full two-parameter treatment.

We first apply our proposal to the Poisson-GOE transition in the model whose curve $\gamma(\beta)$ is the most different from our ansatz (see panel (a) of Fig. 5): the β -ensemble. We take $M = 1$, that is, we repeat the same procedure as with Fig. 6 but with a significantly less abundant number of data. In Fig. 8 we show these results, and we plot the histogram giving the probability density $P(r)$ in conjunction with both the two-parameter fit corresponding to our model Eq. (5) and the single-parameter fit corresponding to our suggested ansatz Eq. (26) for four different values of the transition inducing parameter. Our main conclusion is that when the statistics do not fulfill ideal conditions, that is, when we are not in possession of a sufficiently high amount of evidence, bin fluctuations dominate and outshine the differences existing between both expressions for the distribution. The robustness of a one-parameter fit when compared with a two-parameter one means that this approach allows for a quantification of the degree of chaos in the system that is indeed comparable to the predictions of Eq. (5) but shows, however, a lot less dependence on fitting uncertainties. Indeed, as can be seen in Table IV, the double-fit is expected to be very badly-conditioned (note the relative error of γ , $\sim 147\%$, for the (b) case), whereas its behavior is much stabilized when the second-parameter dependence is removed and the fit is replaced by our ansatz, which is a single-parameter one. We also observe the effect exemplified by Fig. 7 for the (a) case —namely, that when one is in possession of a typical amount of data the double-fit is ill-conditioned and results coming from it do not actually give a measure of chaoticity; instead, one obtains a visually and numerically similar function $P(r; \beta, \gamma(\beta))$ that comes from varying β at the expense of γ , which is then found to be anomalously small. This phenomenon cannot however take place in the large- N limit. As opposed to the double-fit, our ansatz produces physically expected values of β throughout the entirety of the crossover, and is therefore highly reliable upon.

We next move on to examine the accuracy of the results provided by our ansatz Eq. (26) and put them in comparison with those given by the full distribution Eq. (5). We proceed as follows:

(a) We first take $M = 2000$ and construct a single histogram for each value of q , so as to calculate Eq. (23).

(b) We now take only one realization, $M = 1$, we construct the histogram and find Eq. (23). Subsequently, we average the results over the total number of realizations.

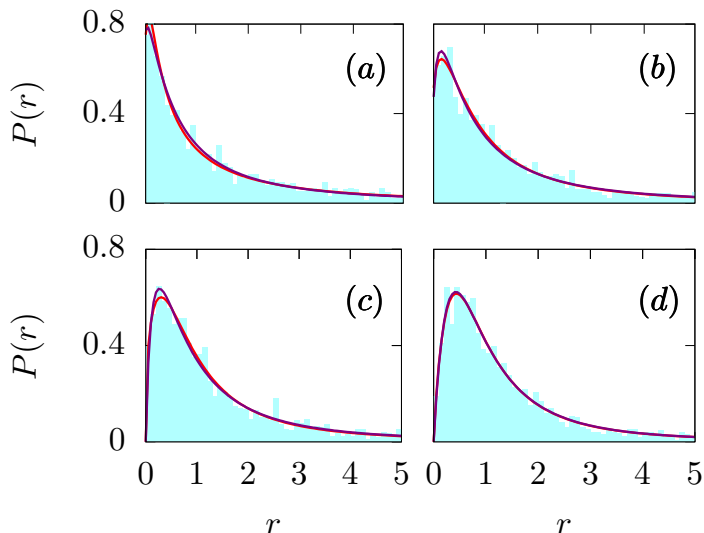


FIG. 8. (Color online) Distribution of the ratio of consecutive level spacings for the β -ensemble model with $N = 1716$, $M = 1$ and $\delta r = 0.1$ (blue, filled histogram), with the best non-linear fits for $P_{\gamma\beta}(r)$, Eq. (5) (red, solid line) and the ansatz $P_{\text{P-GOE}}(r)$ Eq. (26) (purple, solid line). The values of the transition parameter for panels (a) – (d) are given by $q \in \{5, 15, 25, 45\}$, respectively.

Panel	Double-fit	Ansatz
(a)	$\beta = 0.82(23)$ $\gamma = -4.31(14)$	$\beta = 0.234(49)$
(b)	$\beta = 0.38(14)$ $\gamma = 0.44(65)$	$\beta = 0.744(28)$
(c)	$\beta = 0.39(12)$ $\gamma = 1.29(44)$	$\beta = 0.881(16)$
(d)	$\beta = 0.85(21)$ $\gamma = 1.10(48)$	$\beta = 0.9973(83)$

TABLE IV. Values and uncertainties of best non-linear double-fit and with our proposed ansatz referred to panels (a) – (d) in Fig. 8.

For each value of the crossover parameter, we calculate

$$\langle \Delta \rangle_M(q) \equiv \frac{1}{M} \sum_{i=1}^M \left[\frac{1}{n} \sum_{j=1}^n \left| P_H^{(q,i)}(r_j) - P_k^{(q,i)}(r_j) \right|^2 \right], \quad (29)$$

$\forall q \in \{1, 2, \dots, 51\}$, $k \in \{\gamma\beta, \text{P-GOE}\}$, where $P^{(q,i)}(r_j)$

denotes the distribution of the ratio of levels for the i -th realization at $r_j \in [0, 5]$ for the q -th value of the transition parameter. Eq. (29) resolves the issue of incompatibility of data sizes to extract statistical conclusions and permits us in turn to assess the question at hand when statistics is poorer than in our previous simulations, as is in fact often the case.

Application of Eq. (23) and Eq. (29) to the β -ensemble model with $M = 2000$ yields the results shown in panels (a) and (b) of Fig. 9, respectively. Our attention needs to be drawn to two aspects of these findings now.

First, the clear reduction of the difference between the double fit, Eq. (5), and the ansatz, Eq. (26), as the amount of data that originates the distribution decreases. While in both cases one has the same order of magnitude, the procedure of lowering the number of realizations — i.e., averaging over a larger and larger M — causes the two curves to approach each other. Together with Fig. 8, this implies that the transition from integrability to orthogonally invariant chaos can be described either by Eq. (5), for high statistics, or Eq. (26) when one does not have too much data to analyze, which is indeed the point we desired to make. Since a two-parameter fit can become cumbersome and is not practical in many situations, the results lend support to the simpler ansatz option.

Second, the qualitative behavior of $\Delta(q)$ and $\langle \Delta \rangle_M(q)$ deserves proper mention in and of itself. Plots for these quantities differ in that for the first one the curve associated to the ansatz error is quite parabolic while this is no longer the case for the second quantity, where we notice a smooth, nearly constant behavior where increasing monotony is present. This remark should not be taken seriously. As it is, the parabolic behavior is not reached in panel (b) by the curve that corresponds to the ansatz Eq. (26) merely due to fluctuations in the ratios distribution, that manifest more for one-parameter fit when statistics is not abundant that it does for a two-parameter fit, as Eq. (5) requires. For reference, in panel (b) we have also plotted with a blue dashed line the result of applying the same procedure to the theoretical expression $P_W(r; \beta = 1)$, Eq. (11), for the last value of the crossover, corresponding to fully developed GOE. We observe that, in any event, our model Eq. (5) and, more importantly, our ansatz, Eq. (26), yield more precise results.

It should be noted that Fig. 9 provides the final justification for the existence and the choice of such an ansatz as Eq. (26).

VI. OTHER TRANSITIONS

In this section we focus on less typical transitions, the reason for them having been excluded from the previous one being that they do not play so relevant a role in the usually found physical systems that evolve either from regularity to chaos or between different symmetry classes

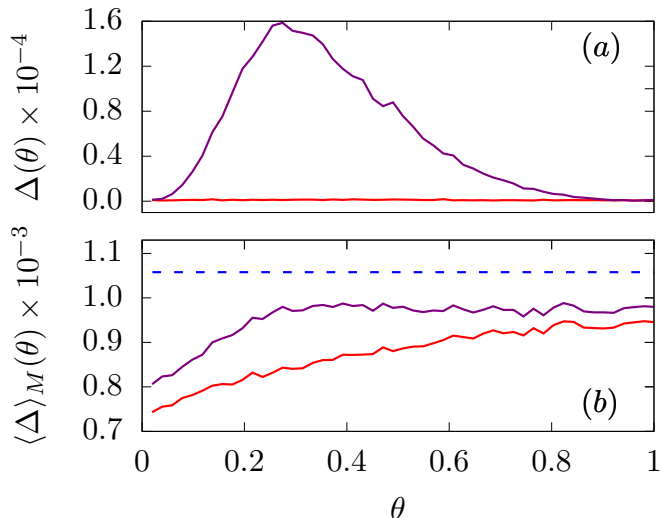


FIG. 9. (Color online) Representation of Eq. (23), panel (a), and Eq. (29), panel (b), for the transiting distribution $P_{\gamma\beta}(r)$, Eq. (5) (red, solid line) and our ansatz suggestion $P_{P-GOE}(r)$, Eq. (26) (purple, solid line) as a function of the value of the normalized transition parameter θ for the β -ensemble model with $M = 2000$ and $N = 1716$. Bin sizes are $\delta r = 0.05$, panel (a), and $\delta r = 0.1$, panel (b). For comparison, we plot in panel (b) the value that the theoretical expression $P_W(r; \beta = 1)$, Eq. (11), would yield when applied to the last (GOE) value of the parameter, $q = 51$, i.e., $\theta = 1$ (blue, dashed line).

within the chaotic regime itself. This is the case for the Poisson-GUE and GOE-GUE transitions. Our purpose is to briefly test the ansatzs we previously proposed for them, bearing in mind that the exact same rationale as that presented for the Poisson-GOE transition is to be followed for its complete justification.

For the Poisson-GUE transition we again make use of an artificially generated system with eigenlevels coming from RMT. We generate the crossover Hamiltonian as

$$\mathcal{H}(\lambda) \equiv \lambda \mathcal{H}_{\text{GUE}} + (1 - \lambda) \mathcal{H}_{\text{P}}, \quad (30)$$

so that $\mathcal{H}(\lambda = 0) = \mathcal{H}_{\text{P}}$ and $\mathcal{H}(\lambda = 1) = \mathcal{H}_{\text{GUE}}$. Here, we have simulated $M = 2000$ realizations consisting of matrices of order $N = 1716$ for each value of $\lambda \in \{1.34^q \times 10^{-6}\}_{q=1}^{50}$. We observe the crossover to happen very fast as λ is increased. After obtaining the histogram $P(r)$ we perform a non-linear fit for our ansatz Eq. (27), and produce the transition that is now shown as visual proof in Fig. 10. Best fit results are also given in Table V. The limiting values of β are in accordance with our expectation.

We observe a perfect match between the histogram distribution and the prediction of our ansatz solution, and find that this covers arbitrarily intermediate steps of the crossover.

In Fig. 11, we assess the error of our ansatz, $P_{P-GUE}(r)$, with respect to the numerical histogram by means of Eq. (29). As usual, for reference we also plot

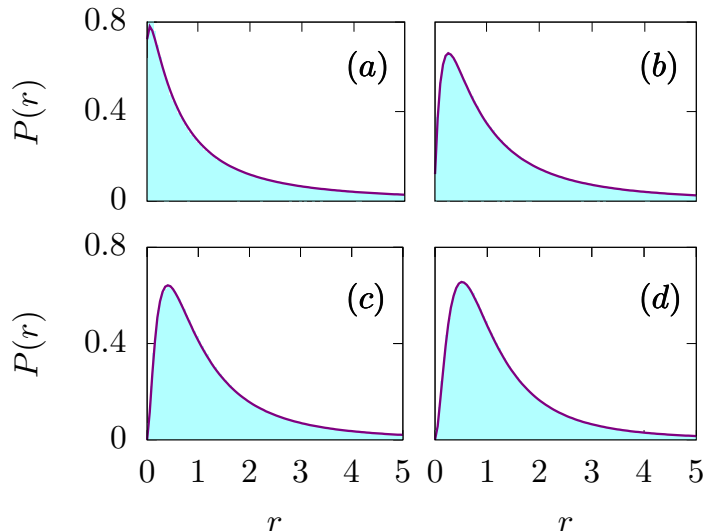


FIG. 10. (Color online) Distribution of the ratio of consecutive level spacings for the RMT transition model with $N = 1716$, $M = 2000$ and $\delta r = 0.05$ (blue, filled histogram), with the best non-linear fit to the ansatz $P_{P-GUE}(r)$, Eq. (27) (purple, solid line). The values of the transition parameter for panels (a) – (d) are given by $q \in \{13, 20, 22, 24\}$, respectively.

Panel	Ansatz
(a)	$\beta = 0.1885(14)$
(b)	$\beta = 1.3798(26)$
(c)	$\beta = 1.7365(34)$
(d)	$\beta = 1.9004(21)$

TABLE V. Values and uncertainties of best non-linear double-fit and with our proposed ansatz referred to panels (a) – (d) in Fig. 10.

with a dashed line the value that results from applying Eq. (29) to the last value of the crossover, thus corresponding to GUE. As we can see, our ansatz is reliable throughout the entire crossover, with a negligible error that never surpasses that of the theoretical GUE distribution for the GUE case.

We finally propose a GOE-GUE crossover generated with RMT. The Hamiltonian is now instead

$$\mathcal{H}(\lambda) \equiv \lambda \mathcal{H}_{\text{GUE}} + (1 - \lambda) \mathcal{H}_{\text{GOE}}, \quad (31)$$

so that $\mathcal{H}(\lambda = 0) = \mathcal{H}_{\text{GOE}}$ and $\mathcal{H}(\lambda = 1) = \mathcal{H}_{\text{GUE}}$. We have simulated following a crossover inducing parameter $\lambda \in \{1.34^q \times 10^{-6}\}_{q=1}^{50}$, and, as before, $M = 2000$ and $N = 1716$. The process is analogous, except we now

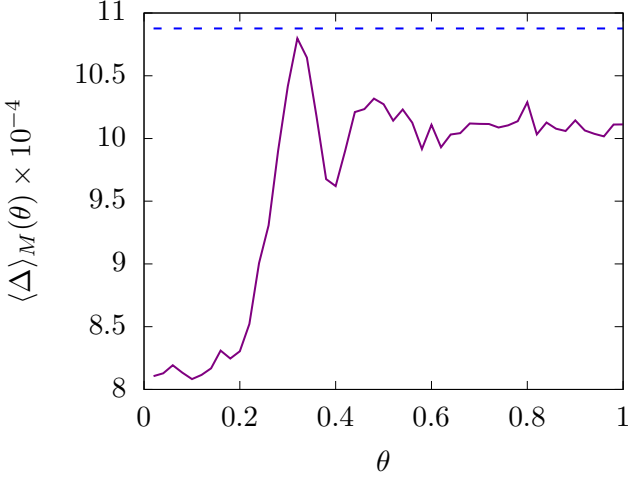


FIG. 11. (Color online) Representation of Eq. (29) for our ansatz suggestion $P_{\text{P-GUE}}(r)$, Eq. (27) (purple, solid line) as a function of the value of the transition parameter θ for the Poisson-GUE crossover Eq. (30) with $M = 2000$ and $N = 1716$. Bin sizes have been taken as $\delta r = 0.1$. For comparison, we plot the value that the theoretical expression $P_W(r; \beta = 2)$, Eq. (11), would yield when applied to the last (GUE) value of the parameter, $q = 50$, i.e., $\theta = 1$ (blue, dashed line).

implement our ansatz Eq. (28). The results can be visually found [45] in Fig. 12, and quantitative results for the β parameter are gathered in Table VI. Analogously, we plot Eq. (29) to study the errors of our ansatz and throughout the crossover and show the results in Fig. 13. Conclusions about the accuracy of the descriptions afforded by this particular ansatz are equivalent to those already given. Indeed, our proposed model seems to give a very good description of the crossover.

Panel	Ansatz
(a)	$\beta = 1.110(12)$
(b)	$\beta = 1.204(13)$
(c)	$\beta = 1.329(12)$
(d)	$\beta = 1.8695(25)$

TABLE VI. Values and uncertainties of best non-linear double-fit and with our proposed ansatz referred to panels (a) – (d) in Fig. 12.

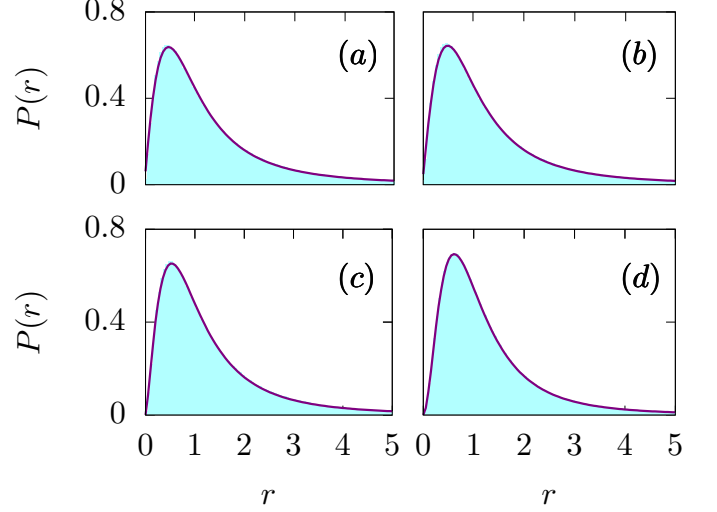


FIG. 12. (Color online) Distribution of the ratio of consecutive level spacings for the RMT transition model with $N = 1716$, $M = 2000$ and $\delta r = 0.05$ (blue, filled histogram), with the best non-linear fit to the ansatz $P_{\text{GOE-GUE}}(r)$, Eq. (28) (purple, solid line). The values of the transition parameter for panels (a) – (d) are given by $q \in \{32, 33, 34, 45\}$, respectively.

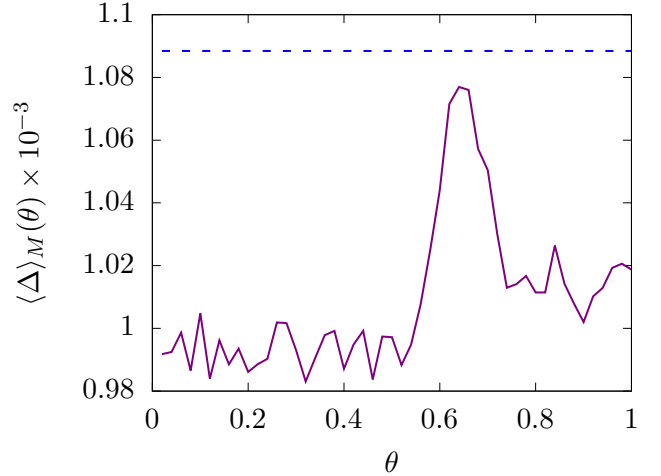


FIG. 13. (Color online) Representation of Eq. (29) for our ansatz suggestion $P_{\text{GOE-GUE}}(r)$, Eq. (28) (purple, solid line) as a function of the value of the normalized transition parameter θ for the Poisson-GUE crossover Eq. (31) with $M = 2000$ and $N = 1716$. Bin sizes have been taken as $\delta r = 0.1$. For comparison, we plot the value that the theoretical expression $P_W(r; \beta = 2)$, Eq. (11), would yield when applied to the last (GUE) value of the parameter, $q = 50$, i.e., $\theta = 1$ (blue, dashed line).

VII. CONCLUSIONS

The distribution of the ratio of consecutive level spacings, a short-range spectral statistic, has been gradually growing in popularity in the recent years since, contrary to the more traditional nearest neighbor spacing distribution, it does not require the unfolding procedure for the analysis. While theoretical expressions for the distribution $P(r)$ are known for the integrable case together with the three classical random ensembles, an analytical interpolating formula between these regularity classes and degrees of chaoticity remains unknown, despite the several attempts having been made in the past.

In this paper, we have proposed a Brody-like interpolating formula that depends on a single parameters, β , and on a function $\gamma(\beta)$ that can be fitted as a second parameter due to our lack of knowledge of its explicit form. This is however *not* to say $\gamma(\beta)$ is actually an independent parameter. Our surmise fulfills the mathematical conditions that are imposed upon such a probability density function. This one-parameter expression is then found to reduce the discrepancy with exact both GOE and GUE simulations with respect to the theoretical expression, which was derived in a Wigner-like spirit, strictly speaking only valid for 3×3 matrices, then by extension applied to arbitrary dimensions.

A central problem in our work has been whether the two-parameter dependence of our crossover model can be reduced to a single-parameter one in such a way that this

still affords a good description of general crossover for physical systems. The answer has been found to be negative. By applying our model to both RMT generated and real physical systems results, we conclude that there cannot exist a universal expression for $\gamma(\beta)$, that is, one that is valid with absolute generality. This is due to the very different natures of the crossover for different systems. Due to the lack of robustness a two-parameter probability density might have for small statistics, we propose ansatz for the main crossovers, Poisson-GOE, Poisson-GUE, and GOE-GUE, for which it can be removed so results can be calculated by means of a single-parameter non-linear fit. These expressions must differ from one another since, as we have already pointed out, there cannot be a general representation for this expression that guarantees universal success in describing crossovers. We show that, so long as the statistics is not huge, which is often the case in the vast majority of situations, employing our ansatz does not result in significant worsening of the description afforded by the statistic $P(r)$ due to fluctuations, which justifies its applicability.

Finally, we show how our proposal can be used for less common transitions with success, such as the Poisson-GUE and the GOE-GUE crossovers.

ACKNOWLEDGMENTS

This work has been supported by the Spanish Grants Nos. FIS2015-63770-P (MINECO/ FEDER) and PGC2018-094180-B-I00 (MCIU/AEI/FEDER, EU).

-
- [1] S. H. Strogatz, *Nonlinear dynamics and chaos*, Perseus books, Readings, Massachusetts (1994).
 - [2] V. I. Arnold. *Mathematical methods of classical mechanics*, Springer-Verlag (1989).
 - [3] J. von Neumann. *Über Funktionen von Funktionaloperatoren*. Ann. Math. **32**, 191 (1931).
 - [4] M. Berry and M. Tabor, *Level clustering in the regular spectrum*, Proc. R. Soc. A **356**, 375 (1997).
 - [5] M. C. Gutzwiller, *Chaos in Classical and Quantum Mechanics*, Springer, New York (1990).
 - [6] E. Wigner, *Characteristic vectors of bordered matrices with infinite dimensions II*, Ann. of Math. **65**, 203-207 (1957).
 - [7] E. Wigner, *On the distribution of the roots of certain symmetric matrices I*, Ann. of Math. **67**, 325-326 (1958).
 - [8] M. L. Mehta, *Random Matrices* (Academic Press, New York, 1991).
 - [9] F. J. Dyson, *Statistical theory of the energy levels of complex systems*, J. Math. Phys. **3**, 140 (1962).
 - [10] O. Bohigas, M. J. Giannoni, and C. Schmit, *Characterization of chaotic quantum spectra and universality of level fluctuation laws*, Phys. Rev. Lett. **52**, 1 (1984).
 - [11] H. J. Stöckmann, *Quantum Chaos* (Cambridge University Press, Cambridge, 1999).
 - [12] E. B. Bogomolny, B. Georgeot, M. J. Giannoni, and C. Schmit, *Chaotic billiards generated by arithmetic groups*, Phys. Rev. Lett. **69**, 1477 (1992).
 - [13] S. Heusler, S. Mller, A. Altland, P. Braun, F. Haake, *Periodic-orbit theory of level correlations*, Phys. Rev. Lett. **98**, 044103 (2007).
 - [14] G. E. Mitchell, A. Richter, and H. A. Weidenmüller, *Random matrices and chaos in nuclear physics: Nuclear reactions*, Rev. Mod. Phys. **82**, 2845 (2010).
 - [15] S. Kumar and A. Pandey, *Random matrix model for Nakagami-Hoyt fading*, IEEE Trans. Inf. Th. **56**, 2360 (2010).
 - [16] G. E. Mitchell, E. G. Bilpuch, P. M. Endt, and J. F. Shriver, *Broken symmetries and chaotic behavior in ^{26}Al* , Phys. Rev. Lett. **61**, 1473 (1988).
 - [17] V. Oganesyan and D. A. Huse, *Localization of interacting fermions at high temperature*, Phys. Rev. B **93**, 041424(R) (2016).
 - [18] C. W. J. Beenakker, J. M. Edge, J. P. Dahlhaus, D. I. Pikulin, S. Mi, and M. Wimmer, *Wigner-Poisson statistics of topological transitions in a Josephson junction*, Phys. Rev. Lett. **111**, 037001 (2013).
 - [19] L. Muñoz, R. A. Molina, J. M. G. Gómez, and A. Heusler, *Examination of experimental evidence of chaos in the bound states of ^{208}Pb* , Phys. Rev. C, **95**, 014317 (2017)
 - [20] J. M. G. Gómez, R. A. Molina, A. Relaño, and J. Retamosa, *Misleading signatures of quantum chaos*, Phys. Rev. E **66**, 036209 (2002).

- [21] A. L. Corps and A. Relaño, *Stringent test on power spectrum of quantum integrable and chaotic systems*, arXiv:1908.09285v2 [quant-ph] (2019).
- [22] V. Oganesyan and D. A. Huse, *Localization of interacting fermions at high temperature*, Phys. Rev. B **75**, 155111 (2007).
- [23] Y. Y. Atas, E. Bogomolny, O. Giraud, and G. Roux, *Distribution of the ratio of consecutive level spacings in random matrix ensembles*, Phys. Rev. Lett. **110**, 084101 (2013).
- [24] A. Sarkar, M. Kothiyal, and S. Kumar, *Distribution of the ratio of two consecutive level spacings in orthogonal to unitary crossover ensembles*, arXiv:1907.07548v1 [math-ph] (2019).
- [25] N. D. Chavda, H. N. Deota, and V. K. B. Kota, *Poisson to GOE transition in the distribution of the ratio of consecutive level spacings*, Phys. Lett. A, **378** (2014) 3012-3017.
- [26] N. D. Chavda and V. K. B. Kota, *Probability distribution of the ratio of consecutive level spacings in interacting particle systems*, Phys. Lett. A, **377** (2013) 3009.
- [27] T. A. Brody, *A statistical measure for the repulsion of energy levels*, Lett. Nuovo Cimento **7**, (1973) 482.
- [28] In actuality, this terminology is borrowed from the NNSD, where one considers the *difference* between consecutive levels in the spectrum. However, for the distribution of the ratio of consecutive level spacings, the equivalent role is played by the *quotient* of these energy differences, making the term *repulsion* a lot less meaningful, at least in its original sense. The link between level repulsion and a quotient of energies is arguably imprecise.
- [29] In any event, we have meticulously checked that the model that implements the transition plays no significant role to our purposes and no qualitative modifications occur as far as our surmise is concerned, which makes the matter irrelevant.
- [30] P. J. Forrester, *Log-gases and random matrices*, London Mathematical Society Monographs, Vol. 34 (Princeton University Press, Princeton and Oxford, 2010).
- [31] I. Dumitriu and A. Edelman, J. Math. Phys. **43**, 5830 (2002); I. Dumitriu and A. Edelman, Ann. Inst. Henri Poincaré, Sect. A **41**, 1083 (2005).
- [32] A. Relaño, L. Muñoz, J. Retamosa, E. Faleiro, and R. A. Molina, *Power spectrum characterization of the continuous Gaussian ensemble*, Phys. Rev. E, **77**, 031103 (2008).
- [33] G. LeCaër, C. Male, and R. Delannay, *Nearest-neighbor spacing distributions of the β -Hermite ensemble of random matrices*, Physica (Amsterdam) **383A**, 190 (2007).
- [34] W. Buijsman, V. Cheianov, and V. Gritsev, *Random matrix ensemble for the level statistics of many-body localization*, Phys. Rev. Lett. **122**, 180601 (2019).
- [35] Although a continuous number of degrees of freedom $k(\beta) \equiv (N-i+1)\beta \in \mathbb{R}_+$, $\forall i \in \{1, 2, \dots, N-1\}$ can seem counterintuitive and lacking sense at first, the probability density function $P_\chi(x; k(\beta))$, $x \in [0, +\infty)$, associated with the random variable $\chi_k(x; k(\beta))$ is *not* ill-defined, and one has $\int_0^\infty dx P_\chi(x; k(\beta)) = 1$, $\forall \beta \in \mathbb{R}_+$, nonetheless, which erases every apparent contradiction.
- [36] I. Bloch, J. Dalibard, and W. Zwerger, *Many-body physics with ultracold gases*, Rev. Mod. Phys. **80**, 885 (2008).
- [37] J. Simon, W. S. Bakr, R. Ma, M. E. Tai, P. M. Preiss, and M. Greiner, *Quantum simulation of antiferromagnetic spin chains in an optical lattice*, Nature **472**, 307 (2011).
- [38] S. Trotzky, Y. A. Chen, A. Fleisch, I. P. McCulloch, U. Schollwöck, J. Eisert, and I. Bloch, *Probing the relaxation towards equilibrium in an isolated strongly correlated one-dimensional Bose gas*, Nat. Phys. **8**, 325 (2012).
- [39] L. F. Santos, *Integrability of a disordered Heisenberg spin-1/2 chain*, J. Phys. A: Math. Gen. **37** (2004) 4723-4729.
- [40] M. Serbyn and J. E. Moore, *Spectral statistics across the many-body localization transition*, Phys. Rev. B **93**, 041424 (2016).
- [41] G. Ortiz, R. Somma, J. Dukelsky, and S. Rombouts, *Exactly-solvable models derived from a generalized Gaudin algebra*, Nucl. Phys. B **707**, 421 (2005).
- [42] J. Dukelsky, S. Pittel, and G. Sierra, *Exactly-solvable Richardson-Gaudin models for many-body quantum systems*, Rev. Mod. Phys. **76**, 643 (2004).
- [43] A. Relaño, *Thermalization in an interacting spin system in the transition from integrability to chaos*, J. Stat. Mech. (2010) P07016.
- [44] M. K. Gould, Y.-Z. Zhang, and S.-Y. Zhao, *Elliptic Gaudin models and elliptic KZ equations*, Nucl. Phys. B **630**, 492 (2002).
- [45] Shown values of q for the Poisson-GUE and GOE-GUE crossovers differ significantly. The choice has been made to reflect the fact that for the former the transition occurs much faster than for the latter. This is due to the scales of non-zero random numbers present in each random matrix—indeed, it is N for Poissonian matrices while it is N^2 for GOE and GUE matrices. This means the Poisson-GOE Hamiltonian quickly changes regime as GUE random numbers are introduced while it takes higher values of the mixing parameter for this modification to manifest in the GOE-GUE crossover. The same would be true for the Poisson-GOE case.